Available online at www.sciencedirect.com
SCIENCE DIRECT®
Physica B 351 (2004) 178–183
PHYSICA B
www.elsevier.com/locate/physb

The electrical properties and the interfaces of Cu_2O/ZnO/ITO p–i–n heterojunction

D.K. Zhang[a], Y.C. Liu[a,b,*], Y.L. Liu[b], H. Yang[a]

[a] *Center for Advanced Optoelectronic Functional Material Research, Northeast Normal University, Changchun 130024, PR China*
[b] *Key Laboratory of Excited State Process, Changchun Institute of Optics, Fine Mechanics and Physics, Chinese Academy of Sciences, Changchun 130022, PR China*

Received 8 January 2004; received in revised form 2 April 2004; accepted 3 June 2004

Abstract

A Cu_2O/ZnO/ITO p–i–n heterojunction was fabricated by electrochemical deposition method. The electrical properties of the p-Cu_2O/i-ZnO/n-ITO heterojunction were studied using the current–voltage measurements. A distinct junction characteristic was observed. Here, the forward and reverse turn-on voltages were about 0.53 and −0.60 V, respectively. An energy-band diagram was proposed to analyze the electrical properties. In terms of the results of the current–voltage measurements, it was deduced that the turn-on voltage was smaller than the barrier potential, which was ascribed to the existence of the interface defect states. The mechanism of charge transportation was discussed and a tunnel recombination process was proposed to explain its electrical properties.

PACS: 78.55. Hx; 73.40.Lq; 68.35.Ct

Keywords: Zno; Cu_2O; Heterojunction; Interface

1. Introduction

Transparent conducting oxides (TCOs) are widely used as transparent electrodes in flat panel displays, optoelectronic devices and solar cells. Zinc oxide (ZnO), a wide direct band gap semiconductor with a band gap energy of ~3.3 eV and a large exciton binding energy of 60 meV, is a good candidate among the transparent conducting oxide thin films. It has been applied in various electrical and optical devices, such as solar cells, room-temperature optically pumped lasing of ZnO in the blue and UV range and blue light emitter diodes [1–3]. However, it is the bottleneck for the practical applications of ZnO to prepare high-quality p-type ZnO semiconducting material. So, it is difficult to construct ZnO homojunction structure [4]. Till now, besides seeking an effective method to prepare p-type ZnO, another route to fabricate high-quality

*Corresponding author. Centre for Advanced Optoelectronic Functional Material Research, Northeast Normal University, Changchun 130024, PR China. Tel.: +86-431-5269168; fax: +86-431-5684009.
E-mail address: ycliu@nenu.edu.cn (Y.C. Liu).

0921-4526/$ - see front matter © 2004 Elsevier B.V. All rights reserved.
doi:10.1016/j.physb.2004.06.003

heterojunction has become attractive. Moreover, heterostructure-based devices exhibit improved carriers confinement compared to homojunctions, which leads to high device performance. One interesting heterojunction is the semiconductor/transparent conducting oxide/ITO p–i–n heterojunctions. Such p–i–n heterojunctions have the merits of high speed, cheaper, low operation voltage, easy fabrication processes and low-dark current. In particular, the report of p-type conductivity in transparent $CuAlO_2$ films [5] has attracted much attention. The reason is that this p-type film can combine with n-type transparent conducting oxides such as ZnO to form heterojunction, which provide a route for the realization of transparent electronic and optoelectronic devices.

It is also known that $CuAlO_2$ related materials such as $CuYO_2$ and $CuScO_2$ families are the transparent conductive oxides exhibiting p-type conductivity [6,7]. Several similar p-type compounds, having the delafossite structure of $CuAlO_2$, have been developed recently [6], according to the guidelines for energy band engineering. Among these semiconductor materials, Cu_2O, having the similar electronic structure with these TCOs, is selected as the p-type semiconductor in this study. This is because Cu_2O, a natural p-type metal oxide with an energy band gap of 2.1 eV and a cubic crystal structure, is usually used in the rectification of alternating current [8]. Moreover, the processing technique used to fabricate this material is relatively simple and low cost. In this study, we prepared Cu_2O/ZnO/ITO p–i–n heterojunction using electrochemical deposition method. Compared with other processes, electrodeposition method presents several advantages such as: low-temperature processing, arbitrary substrate shapes, controllable film thickness and morphology and potentially low cost [9–11].

Although there have been much effort to study the electrical and optical properties of p–i–n heterojunction [12,13], only a few attempts have been performed to investigate the mechanism of charge transportation based on the energy band structure. In the fabrication of heterojunctions, it should be mentioned that there are a large number of lattice defects at the interface that degrade the electrical performance of the devices. Besides, their effect on the charge transportation mechanism has been seldom clearly analyzed. Here, we propose the energy band diagram for the Cu_2O/ZnO/ITO p–i–n heterojunction to explain the electrical properties and analyze the influence of the interface defect states.

2. Experiments

The Cu_2O/ZnO/ITO p–i–n heterojunction was fabricated by electrochemical deposition method. The experimental processes were developed in two steps. The first step is the electrochemical deposition of ZnO films on ITO substrate. The electrochemical deposition was accomplished in a three-electrode electrochemical cell containing aqueous solutions of 0.005 mol/*l* $ZnCl_2$ and 0.1 mol/*l* KCl. KCl was introduced to ensure a good conductivity of the solution. O_2 was bubbled at 0.05 l/min continuously during the deposition process. Commercial conducting glass coated with ITO was used as a working electrode. Prior to film deposition, ITO glass substrates were ultrasonically cleaned in a liquid acetone bath then dipped into a solution of alcohol for a period of 5 min and rinsed with distilled water. The counter electrode was a platinum sheet and an Ag/AgCl electrode was used as the reference electrode. Electrodeposition was controlled at −600 mV vs Ag/AgCl electrode for 1 h by a potentiostat/galvanostat.

The second step is the electrochemical deposition of Cu_2O onto the ZnO film. The deposition setup is the same with that of ZnO. The deposition solution contained 0.4 mol/*l* anhydrous cupric sulphate ($CuSO_4$), 3 mol/*l* lactic acid ($C_3H_6O_3$) and 4 m/l sodium hydroxide (NaOH). $CuSO_4$ was dissolved first in distilled water giving it a light blue color. $C_3H_6O_3$ was then added. Finally, the NaOH solution was added, changing the color of the solution to dark blue with PH = 10. The potentiostatic potential is at −300 mV versus Ag/AgCl electrode. The solution was kept at a constant temperature of 60°C in a controlled temperature water bath during the deposition process for 1 h. The thin-film thickness of

Cu_2O and ZnO were about 4 μm and 300 nm, respectively.

The structural properties were studied by X-ray diffraction XRD using a D/max-rA X-ray diffraction spectrometer (Rigaku) with a Cu K_α line of 1.5418 Å. The optical absorption spectra were investigated on a UV-360 spectrophotometer (Shimadzu). The cross-sectional morphology of the heterojunction was probed by a Hitachi S4200 field-emission scanning electron microscopy (SEM). The electrical characteristics of the Cu_2O/ZnO/ITO p–i–n heterojunction were studied by measuring the current–voltage curves.

3. Results and discussion

Fig. 1 shows the XRD results of the p-Cu_2O/i-ZnO/n-ITO heterojunction. The diffraction peaks of Cu_2O and ZnO are both observed. The XRD spectrum indicates a ZnO peak with (0 0 2) preferential orientation and four Cu_2O peaks at (1 1 0), (1 1 1), (2 2 0) and (2 0 0), respectively. The analysis indicates that Cu_2O used in this study is polycrystalline with a random distribution of cuprous oxide single crystal. The amount of single crystal orientated in the (1 1 1) Miller index is dominant. As shown in Fig. 1, the (0 0 2) peak of ZnO is weaker than the peaks of Cu_2O in intensity, which should be due to that the ZnO layer is below the Cu_2O layer. To confirm the presence of ZnO, the XRD measurements of the single ZnO film grown onto the ITO substrate are shown in the inset of Fig. 1 and the (0 0 2) orientation of the hexagonal crystal structure is strong.

The optical properties of the ZnO and Cu_2O films grown on ITO substrate are investigated by measuring the transmission spectra at room temperature, which is shown in Fig. 2a. According to the transmission spectra, the optical band gaps of ZnO and Cu_2O can be determined. The method based on the relation [14]

$$(\alpha h\nu)^2 = A(h\nu - E_g) \quad (1)$$

is used, where α is the absorption coefficient and $h\nu$ is the photon energy. Fig. 2b shows $(\alpha h\nu)^2$ versus $h\nu$ for the ZnO and Cu_2O films. The energy band gap, E_g, is obtained by linear extrapolation to the $h\nu$-axis. From Fig. 2b, it is found that the energy band gaps of ZnO and Cu_2O are 3.39 and 2.17 eV, respectively, which are in agreement with what have been reported previously [15,16].

Based on the measured band gaps of ZnO and Cu_2O, we present the energy-band diagram of the

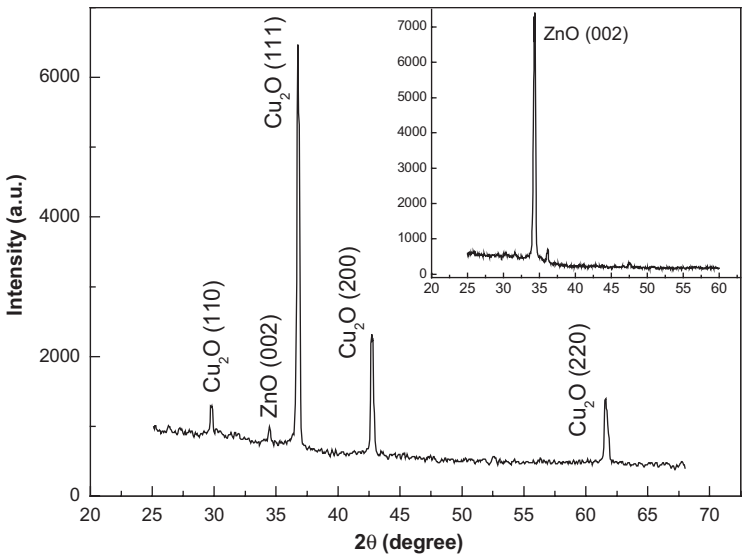

Fig. 1. The XRD spectrum of the Cu_2O/ZnO/ITO p–i–n heterojunction. The inset is the XRD spectrum of the single ZnO film on ITO substrate.

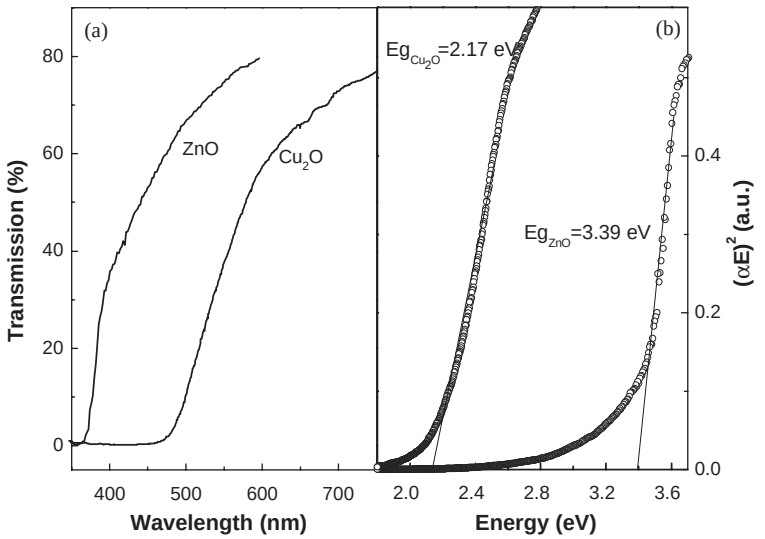

Fig. 2. (a) The transmission spectra of ZnO and Cu_2O films grown on the ITO substrate. (b) Graphical determination of the optical band gap from the transmission spectra of ZnO and Cu_2O grown on the ITO substrate.

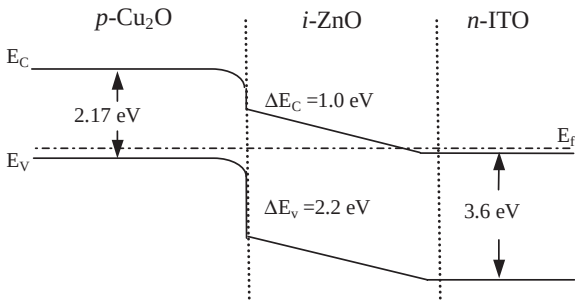

Fig. 3. Energy-band diagram for the Cu_2O/ZnO/ITO p–i–n heterojunction in equilibrium.

heterojunction so as to have a better understanding of the $I-V$ characteristics. An approximate equilibrium energy-band diagram for the transparent Cu_2O/ZnO/ITO p–i–n heterojunction is shown in Fig. 3 [6]. Cu_2O is a p-type semiconductor with an electron affinity of 3.2 eV [17] and ZnO (conductivity $\sigma = 24.5\,S\,cm^{-1}$) is semi-insulating layer with an electron affinity of 4.2 eV [18], respectively. ITO with a band gap of $\sim$3.6 eV [19] is a degenerately doped n-type TCO, so its Fermi level, E_F, is positioned slightly above the conduction-band minimum, E_C. The work function of ITO is $\sim$4.7 eV [20]. ΔE_C and ΔE_V denote the differences in conduction bands and valence bands of Cu_2O and ZnO, respectively. It can be calculated that $\Delta E_C = 1.0\,eV$ and $\Delta E_V = 2.2\,eV$. As the three materials are brought into contact, a constant Fermi-level will be formed at equilibrium. This is accomplished when electrons in the n-ITO are transferred to the p-Cu_2O through the i-ZnO layer and holes are transferred in the opposite direction until the Fermi-level is aligned.

Three noteworthy features of the energy-band diagram merit further comment. First, the barrier for charge injection is formed mainly at the p–i interface, due to the significant mismatch in band gaps between Cu_2O and ZnO. Second, the p-Cu_2O/i-ZnO/n-ITO heterojunction exhibits a small conduction band discontinuity along with a large valence band discontinuity. This heterojunction structure offers an easy way for electron injection from the n-type ITO to the p-type Cu_2O and blocks back hole injection from the p-to-n side under the forward applied voltage. Third, the semi-insulated ZnO layer makes the energy band between Cu_2O and ITO smoother. Such ZnO layer decreases interfacial conduction-and valence-band discontinuities and results in an easier transition between bulk energy bands of Cu_2O and ITO.

To measure the $I-V$ characteristics of the p-Cu_2O/i-ZnO/n-ITO heterojunction, semitransparent Au thin films the work function of which is 5.2 eV similar with that of Cu_2O and ITO have been evaporated on the top faces of the Cu_2O and ITO layers to make ohmic contact, respectively. The schematic structure of the p–i–n heterojunction is illustrated in the inset of Fig. 4.

Typical $I-V$ curve for the Cu_2O/ZnO/ITO p–i–n heterojunction is shown in Fig. 4. Such resultant Cu_2O/ZnO/ITO heterojunction exhibits distinct junction characteristic. The turn-on voltages are ~ 0.53 and ~ -0.60 V for forward and reverse bias, respectively. It is obvious that the turn-on voltages are smaller than the barrier potentials obtained from energy-band analysis. It should be attributed to the existence of many interface defect states in the p–i–n heterojunction. As ZnO and Cu_2O contact, the energy spike and potential well constitute an energy barrier. In general, an electron that travels from the n-to-p side must climb the barrier, which needs a higher applied voltage. Due to the large mismatch of the lattice constant between ZnO and Cu_2O, there must be many interface states in the depletion layer, which can play an important role in the charge transportation process. If a positive voltage is gradually applied to the p side with respect to the n side, the potential barrier becomes decreasing, the depletion layer gets narrower and the band edge become sharper. When the applied voltage reaches a critical value, the conduction-band minimum of ZnO is higher than the interface state levels. Electrons from the conduction band of ITO may tunnel through the junction potential barrier into the empty interface states and then transfer into the valence band of Cu_2O to produce a current, without climbing the barrier. It is the tunnel recombination process, as shown in Fig. 5. Under the negative voltage, the energy band of ITO drops and that of Cu_2O rises. Because of the existence of interface states, holes in the valence band of Cu_2O are easily transferred from the p-to-n side tunneling through the junction potential barrier.

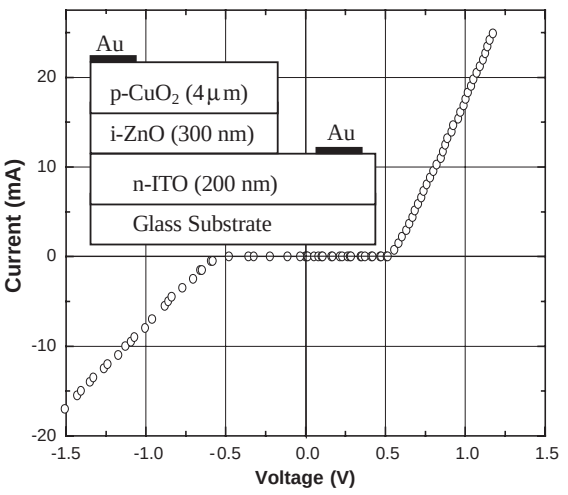

Fig. 4. $I-V$ characteristics for Cu_2O/ZnO/ITO p–i–n heterojunction. The inset is schematic structure of the heterojunction used for measuring the $I-V$ characteristics.

To confirm the presence of the high-interface states, we calculate the lattice mismatch given by the relation [21]

$$\frac{\Delta a}{a} = \frac{2(a_2 - a_1)}{a_2 + a_1} \tag{2}$$

and the dangling bond density, which is given by the relation [21]

$$N_{st} = \frac{a_2^2 - a_1^2}{a_1^2 a_2^2}, \tag{3}$$

where a_1, a_2 are the lattice constant of ZnO and Cu_2O, respectively. The lattice mismatch between the two lattices is 27.1% according to formula (2) and the dangling bond density is $3.99 \times 10^{18}\,cm^{-2}$ according to formula (3) ($a_1 = 3.249$ Å, $a_2 = 4.269$ Å), which are higher than those of most materials such as Ge/Si heterojunction with the mismatch of 4.1% and the dangling bond density of $1.1 \times 10^{14}\,cm^{-2}$ [22]. So the large lattice mismatch leads to a large interface defect states.

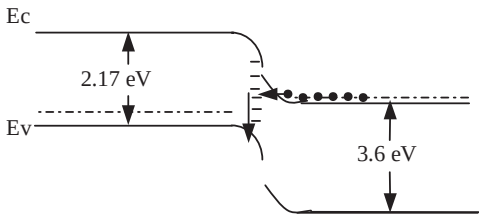

Fig. 5. Energy-band diagram for the Cu_2O/ZnO/ITO p–i–n heterojunction under forward applied voltage.

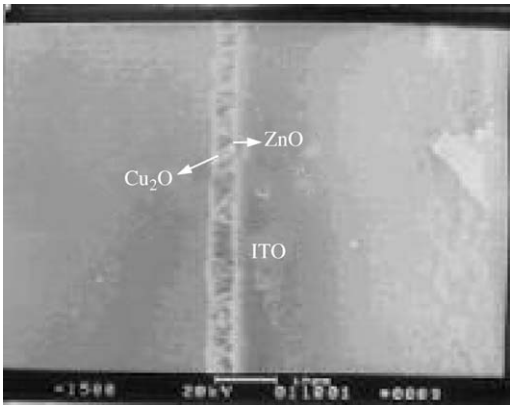

Fig. 6. The cross-sectional SEM image of Cu_2O/ZnO/ITO p–i–n heterojunction.

Another evidence is from the cross-sectional SEM image, as shown in Fig. 6. The thin-film thickness of Cu_2O and ZnO could be measured about 4 μm and 300 nm, respectively. From the cross-sectional image, a clear interface structure is observed near the interface betweem Cu_2O and ZnO layers. Though the XRD result reveals that Cu_2O and ZnO crystallites are formed in the heterojunction, there are still many crystal boundaries in the interface of Cu_2O and ZnO. This further confirms the existence of the interface states that influence the charge transportation mechanism.

4. Conclusion

The Cu_2O/ZnO/ITO p–i–n heterojunction has been successfully fabricated using an inexpensive and simple method of electrochemical deposition. The electrical properties of the p-Cu_2O/i-ZnO/n-ITO heterojunction are obtained using the current–voltage measurements. The p–i–n heterojunction exhibits a distinct junction property. We propose the energy band diagram for the heterojunction to explain the electronic mechanisms. The smaller turn-on voltage is due to the tunnel recombination process that is based on the existence of the interface defect states in Cu_2O and ZnO.

Acknowledgements

This work was supported by the National Natural Science Foundation of China (60176003, 60376009), and the Foundational Excellent Researcher to Go beyond Century of Ministry of Education of China.

References

[1] H. Hiramatsu, K. Imaeda, H. Horio, M. Nawata, J. Vac. Sci. Technol. A 16 (1998) 669.
[2] M. Joseph, H. Tabata, T. Kawai, Appl. Phys. Lett. 74 (1999) 2534.
[3] H. Fabricius, T. Skettrup, P. Bisgaard, Appl. Opt. 25 (1986) 2764.
[4] D.C. Look, Abstract booklet, in: Second International Workshop on Zinc Oxide, Wright State University, Dayton, 2002.
[5] H. Kawazoe, M. Yasukawa, H. Hyodo, M. Kurita, H. Yanagi, H. Hosono, Nature (London) 389 (1997) 939.
[6] R.L. Hoffman, J.F. Wager, M.K. Jayaraj, J. Tate, J. Appl. Phys. 90 (2001) 5763.
[7] N. Duan, A.W. Sleight, M.K. Jayaraj, J. Tate, Appl. Phys. Lett. 77 (2000) 1325.
[8] K. Othmer, Encyclopedia Chem. Technol. 4 (1963) 472.
[9] J.A. Switzer, R. Liu, E.W. Bohannan, F. Ernst, J. Phys. Chem. B 106 (2002) 12369.
[10] Z.H. Gu, T.Z. Fahidy, J. Electrochem. Soc. 146 (1999) 156.
[11] D. Gal, G. Hodes, D. Lincot, H.W. Schock, Thin Solid Films. 361–362 (2000) 79.
[12] J. Furlan, F. Smole, P. Popovic, M. Topic, M. Kamin, Sol. Energy. Mater. Sol. Cells. 53 (1998) 15.
[13] C.C. Chang, S.J. Lii, Solid State Electron. 42 (1998) 817.
[14] M. Tapiero, C. Noguet, J.P. Zielinger, C. Schwab, D. Pierrat, Rev. Phys. Appl. 14 (1979) 231.
[15] V. Srikant, D.R. Clarke, J. Appl. Phys. 83 (1998) 5447.
[16] A.E. Rakhshani, Solid State Electron. 29 (1986) 7.
[17] W. Siripala, A. Ivanovskaya, T.F. Jaramillo, S.H. Baeck, E.W. McFarland, Sol. Energy. Mater. Sol. Cells. 77 (2003) 229.
[18] H. Kobayashi, H. Mori, T. Ishida, Y. Nakato, J. Appl. Phys. 77 (1995) 1301.
[19] T. Minami, T. Miyata, T. Yamamoto, Surf. Coat. Technol. 108–109 (1998) 583.
[20] J.R. Sheats, H. Antoniadis, M. Hueschen, W. Leonard, J. Miller, R. Moon, D. Roitman, A. Stocking, Science. 273 (1996) 884.
[21] L.S. Yu, in: Y.F. Li (Ed.), Physics of Semiconductor Heterojunction, Science Press, Beijing, 1990.
[22] R. Dornhaus, G. Nimtz, Narrow-gap semiconductor, Springer Tracts Mod. Phys. 98 (1983) 164.